Granular Matter (2017) 19:23
DOI 10.1007/s10035-017-0708-7

ORIGINAL PAPER

Segregation due to particle shape of a granular mixture in a slowly rotating tumbler

G. G. Pereira[1] · **P. W. Cleary**[1]

Received: 9 November 2016

Abstract Using DEM particle simulations we consider segregation of a binary granular particle mixture in a slowly rotating cylindrical tumbler where the particles differ only in their shape—spherical versus more cubical particles. We find that the more cubical particles segregate to the inner core of the particle bed while the spherical particles segregate to the curved walls of the tumbler. The main mechanism for this segregation is different energy dissipation rates for the different particle shape types when avalanching down along the free surface. The cubical particles, due to their sharper corners, dissipate energy much faster than the spherical particles. This results in spherical particles reaching the bottom end of the sloped, free surface which are then transported around the cylinder adjacent to the cylinder wall, as rigid body motion. In contrast to size or density segregation, the segregation due to shape is much weaker and takes longer to reach its equilibrium or steady state. In addition, the segregation occurs *along* the top surface rather than *through* the top surface (as occurs for size and density segregation). In general, in situations where two particles differ in their ease of flow (viz *flowability*) the more rapidly flowing particle will segregate to the base of the free surface (which in the case of the tumbler results in spherical particles near the periphery) and the more slowly flowing particle will segregate underneath.

Keywords Segregation · Particle shape · Rotating tumbler · Discrete element method

✉ G. G. Pereira
Gerald.Pereira@csiro.au

[1] CSIRO Computational Modelling, Private Bag 10, Clayton South 3169, Australia

1 Introduction

Granular mixtures made up of particles which differ in size, density and/or shape tend to segregate when flowing, vibrating or are being sheared [1]. These granular mixtures are not only important industrially, but have great scientific richness, which has yet to be understood fully. Consider a granular mixture consisting of two different particle types (*binary mixture*), which is placed in a cylindrical tumbler. If the tumbler is approximately half-filled with this mixture and rotates about its axis, which is perpendicular to the gravity vector, then a core of dense (or small) particles results. The physical mechanisms behind the formation of such a core pattern are now well understood with good agreement between theory, simulations and experiments [2–18]. Smaller particles tend to percolate down into the core, through the interstitial voids between particles, while denser particle sink through the particle bed into the core—a mechanism called buoyancy.

The idealized situation of purely spherical particles is more easily modelled than the case where particles have some non-spherical shape. Certainly with respect to Discrete Element Method (DEM) simulations, determining contact points between non-spherical particles is a much more complex task than for spherical particles. See the recent review article by Lu, Third and Muller [19] which details these complexities and methodologies to treat the non-spherical case. However, it is well known particle shape is an important intrinsic particle property which can lead to a variety of fundamental and interesting macroscopic differences to granular mixtures composed of purely spherical particles. In this paper, we would like to understand how particle shape (specifically blocky particles such as cubes) can affect segregation in binary granular mixtures which are slowly rotated in a cylindrical tumbler.

Published online: 07 March 2017

Whereas there is quite an abundance of both experimental and theoretical work on mixing and segregation of mixtures of particles which may differ either in their size or even their density, there is significantly less work on segregation of particle mixtures where particles differ in shape. Through experiments, Pollard and Henein [20] looked at kinetics of radial segregation of different sized but irregularly shaped particles in slowly rotating cylindrical tumblers. They concentrated on the rate of segregation and found this was dependent on the tumbler's rotational speed and also the particle size ratio. Moreover, they found the segregation core contained more of the larger particles than for similar experiments with spherical particles. They attributed this to the irregular shape of the particles since they are less flowable than spheres. Dube et al. [21] looked at the dynamics of non-spherical particles in rotating drums through experiments. They mainly considered mono-disperse non-spherical particles but briefly considered mixing and segregation in bi-disperse non-spherical particle mixtures. Their results showed particle shape can affect the segregation (or mixing) of bi-disperse granular mixtures in a rotating drum.

Caulkin et al. [22] looked at segregation in vibrating beds using both experiments and simulations. Their experiments consisted of placing bi-disperse granular mixtures in a Hele-Shaw cell (i.e. between two closely spaced, vertical glass plates). The cell was then vibrated gently at which time segregation occurred. Their simulations were a type of cellular automata model. From these experiments the authors concluded the geometry of particles, i.e. aspect ratio, sphericity and size ratio strongly influenced segregation.

The work that is most relevant to our present study is that by Makse and co-workers [23–25]. In their experiments, Makse et al. [23,24] poured a bi-disperse granular mixture into a Hele-Shaw cell causing a heap to form. The particles differed in both size and shape (cubes and spheres). This lead to a variety of segregation patterns including a stratification pattern. Makse [25] went on to propose that segregation in avalanching heaps formed from binary mixtures of cubical and spherical particles will have spherical particles at the bottom and cubical particles at the top. This is because the cubical particles will tend to form heaps with larger angles of repose than the spherical particles. Makse [25] did not explore this segregation in rotating tumblers as he was more concerned with the interplay between shape and size segregation leading to stratification patterns in heaps. However, his thesis that segregation in granular mixtures where particles differ in their shape is driven by differing angles of repose appears the accepted mechanism in the literature.

Pereira et al. [9,14] considered binary mixtures of particles which simultaneously differed in size, density and shape to understand the formation pattern of streaks in a thin, rotating tumbler. Since particles differed in all three main intrinsic properties which are all known to cause segregation, they were not able to precisely determine the mechanisms underlying shape segregation. Wachs et al. [26] looked at the dynamics of a variety of non-spherical particles in rotating tumblers through DEM simulations. The particle shapes included cylinders, cubes and tetrahedrons and showed that avalanching persisted to relatively high rotation speeds for granular beds made of non-spherical particles compared to spherical ones. Hohner et al. [27] implemented polyhedral dices in their DEM simulations of rotating drums and found the dynamic angle of repose increased with increasing angularity of the particles.

While the main mechanisms behind size and density segregation are now generally well accepted, the same cannot be said for shape segregation. Makse's work on segregation in granular heaps, which is closely related to segregation in rotating tumblers, implies the main mechanism for segregation is related to the difference in angles of repose of the two particle types [25]. More rounded particles generally have a smaller angle of repose compared to less rounded particles [28]. Thus his modelling [25] predicts the more rounded particles will be found at the bottom of a granular heap with smaller repose angle and the less rounded particles on the upper parts of the heap leading down from the top with a larger angle of repose. Thus our main goal here is to understand whether and why segregation due to shape occurs in bi-disperse granular mixtures which half-fill a rotating tumbler. Is the repose angle the mechanism behind segregation or are there are other mechanisms behind the granular segregation? We consider relatively slow flows with a Froude number ($Fr \equiv \omega^2 R/g$, where R is the cylinder radius, ω the cylinder rotation speed and g gravity) of the order of 10^{-5} to 10^{-4}, so that the top surface of the particle bed is flat corresponding to the continuous flow regime [1]. We do this through DEM simulations which can virtually probe the particle bed and hence uncover the underlying physics. Many experiments have used sugar-cubes (or similar) in their granular mixtures and so we consider blocky (cubical) particles as our non-round particles.

2 DEM methods and measures

To carry out this study we use a DEM method (using an in-house code) which has been documented a number of times in our previous works [8,9,13,14,28–31]. Very briefly, the method follows the motion of every particle and object in the flow and modelling each collision between the particles and between the particles and their environment. We use a soft contact model to determine collisional forces, where particles are allowed to overlap and the amount of overlap Δx and normal v_n and tangential v_t relative velocities determine the collisional forces via a linear spring dashpot model. Numer-

Table 1 DEM simulations carried out for ratio of shape factors R_n with their final segregation value (i.e. after 180 seconds of rotation), $\Phi_{\alpha\beta}$

R_n	$\Phi_{\alpha\beta}$ (1 rpm)	$\Phi_{\alpha\beta}$ (3 rpm)
1.256	0.0333	0.0440
1.502	0.0826	–
1.749	0.1424	0.2064
1.995	0.1894	–
2.241	0.2512	0.2960
2.488	0.2978	0.3368
3.472	0.3881	0.4005
4.951	0.4272	0.4797

The second column corresponds to results at 1 rpm and third column at 3 rpm

ical values for spring constants and dampers are similar to those given previously [8,9,13,14,29,30].

We use a cylinder of diameter 10 and 2 cm depth with periodic boundary conditions in the z (axial) direction. By using periodic boundary conditions we are attempting to model a long cylinder and so neglect any axial segregation due to end-wall effects, while focusing on the radial segregation. The gravity vector points in the negative y direction. Particles are of density 2595 kg/m^3 with frictional parameters as given in our previous works [8,9,13,14,29,30]. The particles are not spherical but super-quadric (blocky) in shape. Their shape obeys the equation

$$\left(\frac{x}{a}\right)^n + \left(\frac{y}{a}\right)^n + \left(\frac{z}{a}\right)^n = 1, \tag{1}$$

where a is the particle size and n defines the amount of blockiness of a particle. In the following we refer to n as the *shape factor*. When $n = 2$ Eq. (1) yields a sphere of radius a and as $n \to \infty$ it yields a cube with side length $2a$. We use particles with an average size $a = 2$ mm. The computational time increases with increasing n [9,14]. For each set of simulations we have a 50:50 mix of nearly spherical particles ($n = 2.03$) and more blocky particles where n varies from 2.55 up to 10.05 between simulations. Table 1 gives a list of all the shape factor ratios, R_n, used.

Equation (1) which we use to define the shape of the particles in our DEM simulations has been chosen as it naturally transitions from a sphere (when $n = 2$) to a cube (as $n \to \infty$) without varying any other parameters in the equation. The diameter of the sphere is $2a$ while the corresponding cube also has an edge length of $2a$. The mid-points of the cube-faces are tangent to the sphere at six points and the sphere is fully enclosed within the cube. We refer to this particular choice for the sphere as the *inscribed* sphere and has radius a.

A critical issue in setting up a DEM configuration for evaluating shape induced segregation is to try to ensure or at least minimize the effects of size segregation. In order to identify the shape effects, the particles need to have equivalent sizes so that there is minimal size segregation. This requires a definition for what is the equivalent size of a super-quadric particle. For this work we have chosen to define the particle size for a super-quadric shape to be the edge length. Other choices are possible for defining what are equivalent sized particles. For example one could choose equal volume as the basis which means that particles are deemed to have equal sizes if they have the same volume. In this case, the sphere radius corresponding to the equivalent cubic particle would be $(6/\pi)^{1/3}a \approx 1.24a$.

Alternatively, we could choose to have the cube completely contained within the sphere, so that the six vertices of the cube touch the surface of the sphere. We call this the *circumscribed* sphere and in this case the sphere radius is $\sqrt{3}a \approx 1.73a$.

It is, a priori, unclear which is the better choice as a basis for equivalency but we consider the inscribed sphere to be the natural choice. The inscribed sphere is the smallest of the three choices, with the equal volume sphere being slightly larger and the largest being the circumscribed sphere. It is also extremely unlikely that the dynamically equivalent sphere could be smaller than this since it then would be smaller in every direction compared to an equivalently defined super-quadric shape. We will discuss the consequences of this equivalency choice and the dependence of the simulation results on this in the Discussion section.

The Froude number F, defined as $F \equiv \omega^2 R/g$ is a dimensionless number commonly used to determine the regime of the granular flow. For our system, we use rotational speeds of 1–3 rpm which corresponds to a Froude number of 5.6×10^{-5} to 5.0×10^{-4} which puts the flow predominantly in the continuous flow regime (but to the lower end of this regime bordering with the avalanching regime). It should be noted that particle shape is intricately related to the ability to flow so that the two different sets of particles (round or cubical) may display different flow characteristics [32].

We calculate the volume fraction of each particle type, (f_A, f_B) as a function of the distance from the centre of the cylinder (averaged over the axial direction), which we call the *radial distribution function*. To obtain this we divide the cylindrical cross-section into 15 equally spaced annuli and calculate the volume of each type of particle within each annulus (i.e., has its centre located within the annulus). This volume is normalized by the total volume of particles within each annulus, yielding a value between zero and one. Thus we obtain a volume fraction for each particle type which is a function of the scaled distance from the centre of the cylinder (scaled with the cylinder radius). This measurement is taken at the end of the simulations (once the particle distribution is stable and in equilibrium).

We also calculate a measure of overall segregation by dividing the simulation domain into small cubic boxes with

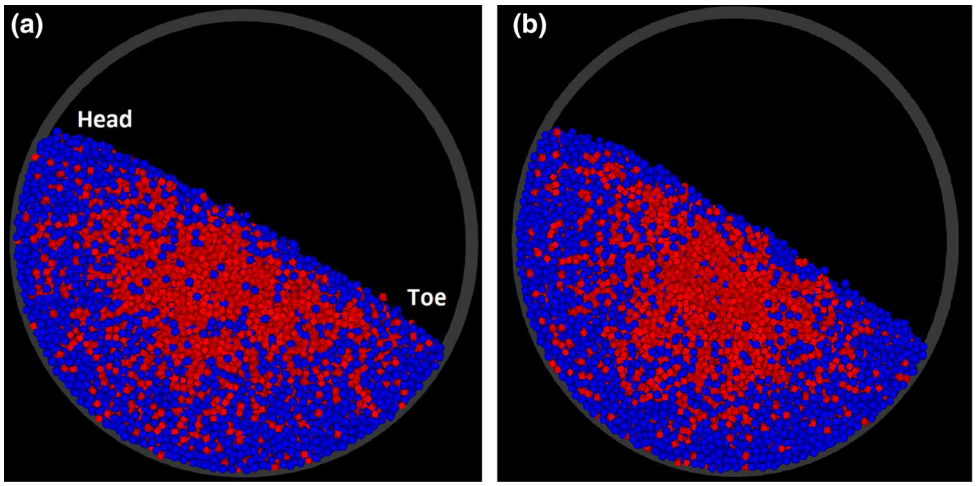

Fig. 1 Particle distribution for binary mixture with particle shape factors of 2.03 (*blue*) and 4.55 (*red*) at two stages during the cylinder's rotation: **a** after 4.5 rotations and **b** after 9 rotations. In **a** we also point out the location of the *head* of the particle bed at the *top* of the flowing layer and the *toe* of the particle bed, at the *bottom* of the flowing layer (color figure online)

an edge length of approximately 5 particle diameters. Then we count the number of each particle type in each of the boxes and calculate the deviation from a perfectly mixed (homogeneous) mixture of particles (i.e., equal volume of each of the components). We use the following definition for segregation (between two components, α and β):

$$\Phi_{\alpha\beta} = \frac{1}{V} \sum_{i=1}^{N_{cell}} \left(V_\alpha(i) - V_\beta(i)\right)^2 V(i) \tag{2}$$

where the total number of small cubes is N_{cell}, V is the total volume of particles in the domain, while volumes in the ith cell are indicated with (i). In a perfectly mixed sample, the volumes of each of the components should be the same in all cells, so that the difference in (2) is zero. Hence $\Phi_{\alpha\beta}$ is zero. For a segregated sample, the difference in (2) is non-zero and so $\Phi_{\alpha\beta}$ will be non-zero. The more segregated the sample is, the larger the numerical value of $\Phi_{\alpha\beta}$. The second factor in the sum in Eq. 2 gives a weighting to cells with more particles in them. The overall $\Phi_{\alpha\beta}$ value is normalized with the maximum segregation value which is calculated by having a single interface between two phases (i.e. 1/4 of container has one type of particle and the other 1/4 has the other type). Thus the final segregation value is between 0.0 and 1.0 [13,14].

3 DEM results

When the cylindrical tumbler rotates at 3 rpm the top interface remains quite flat and the flow is clearly in the continuous flow regime. Consider a binary mixture of particles with a shape factor ratio of 2.241. Figure 1 shows the particle distributions at two times (after 4.5 and 9 rotations) during the segregation process. Clearly the rounder particles (blue) have segregated predominantly to the periphery of the cylinder while the more cubical particles (red) have migrated to the inner (core) region. The interface between components, however, is relatively diffuse, with a few cubical particles appearing near the periphery and, conversely, rounder particles appearing in the inner core region. In comparison, for particles which differ in size or density much sharper interfaces are usually observed [8,13].

The mode of segregation for shape segregation appears to be quite different to that observed for density or size segregation [8,13]. In this case segregation appears to be *along* the surface layer rather than through it. This means we find the segregated region begins to evolve close to the toe end of the bed (with a higher concentration of spherical particles). (The toe end of the bed is at the bottom of the flowing layer and is shown in Fig. 1a.) This high concentration of spherical particles forms a layer adjacent to the cylinder wall as it moves in rigid body rotation with cylinder rotation, from the toe up to the head of the particle bed from which avalanching begins. Over subsequent cylinder rotations, the thickness of this spherical particle layer increases. In contrast, for the case of size or density segregation, segregation occurs *through* the surface layer and thus the segregated region evolves rapidly from just below the bottom of the surface shear layer. Segregation occurs much more slowly for shape segregating in contrast to size or density segregation.

The radial distribution function for this shape factor ratio is shown in Fig. 2a. The maximum value of this distribution function, for the more cubical particles, is 0.82 at a scaled radius of 0.18. Meanwhile for the rounder particles, the maximum occurs at the largest scaled radius of 0.95 with a value of 0.87. Note that the cubical particles do not have their maximum value at a scaled radius of zero because the top flow layer has a mixture of both sorts of particles. The temporal evolution of overall segregation ($\Phi_{\alpha\beta}$) is shown in Fig. 2b. Initially the segregation increases linearly with time (number of rotations) until about 4 rotations at which point the segregation growth levels off, before plateauing at a value of about 0.3. This value represents a relatively moderate amount of segregation. For size and density segregation [13] this mea-

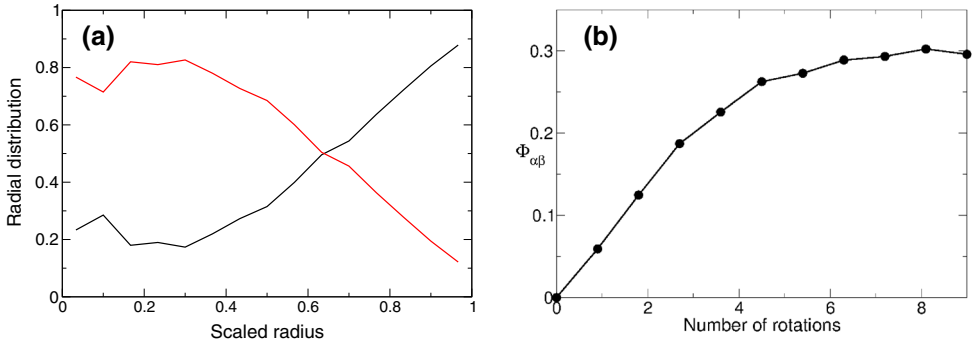

Fig. 2 **a** Radial distribution function for binary mixture with $R_n = 2.241$ after 9 rotations. **b** Segregation measure as a function of number of rotations for binary mixture with $R_n = 2.241$ (color figure online)

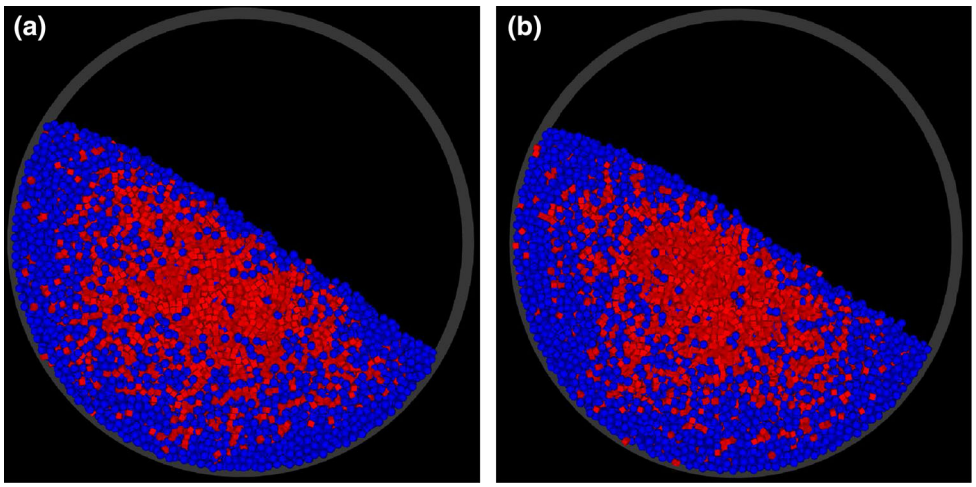

Fig. 3 Particle distribution for binary mixture with particle shape factors of 2.03 (*blue*) and 10.05 (*red*) at two stages during the cylinder's rotation: **a** after 4.5 rotations and **b** after 9 rotations (color figure online)

sure was above 0.6 for most size and density ratios. Also, as mentioned before, the dynamics of segregation is relatively slow with maximum segregation only being reached after around five cylinder rotations. So in general shape segregation appears to be weaker in comparison to size or density segregation.

We now contrast with the case of a binary mixture where the particles have a shape factor ratio of 4.951 for the same cylinder rotation rate of 3 rpm. The particle distribution is shown in Fig. 3. The segregation now is stronger, with the core region having a higher concentration of cubical (red) particles, with very few blue (spherical) particles. The region adjacent to the cylinder wall is now quite highly concentrated with spherical (blue) particles but the interface between these regions remains relatively wide and diffuse, in comparison to size and density segregation [8,13,30].

The radial distribution function and segregation measure for this case (shape factor ratio of 4.951) are shown in Fig. 4. The shape of the radial distribution function is similar to that of the previous case (Fig. 3) but the maxima corresponding to each particle type is slightly larger, which implies better segregation is achieved. For the cubical particles the maximum is around 0.85 while for the spherical particles it is 0.95. The segregation measure also achieves a larger $\phi_{\alpha\beta}$ value of 0.48, which indicates better overall segregation is achieved in this case. The dynamics of segregation is still relatively slow, with the maximum only being achieved after seven rotations.

For comparison to the two previous cases (shape ratios of 2.241 and 4.951), we now consider a smaller size ratio case of $R_n = 1.256$. The particle distributions at two stages during the tumbler rotation are shown in Fig. 5. In contrast to the Figs. 1 and 3, it is clear the core and corona segregation pattern is absent. Blue (spherical) and red (less rounded) particles appear to be quite evenly distributed throughout the particle bed. This is borne out when looking at the radial distribution function in Fig. 6a. Here the maximum value of either phase reaches only about 0.6 - which is only slightly above their overall bulk volume fraction of 0.5. The segregation measure $\phi_{\alpha\beta}$, shown in Fig. 6b, also is very small only reaching 0.044 after 9 rotations of the cylinder. This value is much smaller than the previous cases. In summary segregation is quite weak and very slow for $R_n = 1.256$.

We have run several other cases with a combination of (close to) spherical particles (shape factor 2.03) and more cubical particles with shape factors of 3.05, 3.55, 5.05 and 7.05. The general results are consistent with the three cases we have discussed in detail above. The asymptotic values of the segregation measure ($\phi_{\alpha\beta}$) for all the cases simulated are given in Table 1. We also have repeated these simulations at a lower cylinder rotation rate of 1 rpm. Since we are still in the

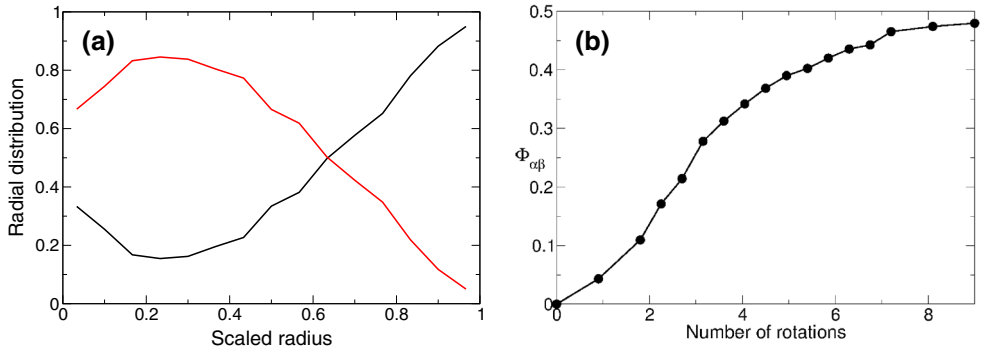

Fig. 4 **a** Radial distribution function for binary particle mixture with $R_n = 4.951$ after 9 rotations. **b** Segregation measure as a function of number of rotations for binary mixture with $R_n = 4.951$ (color figure online)

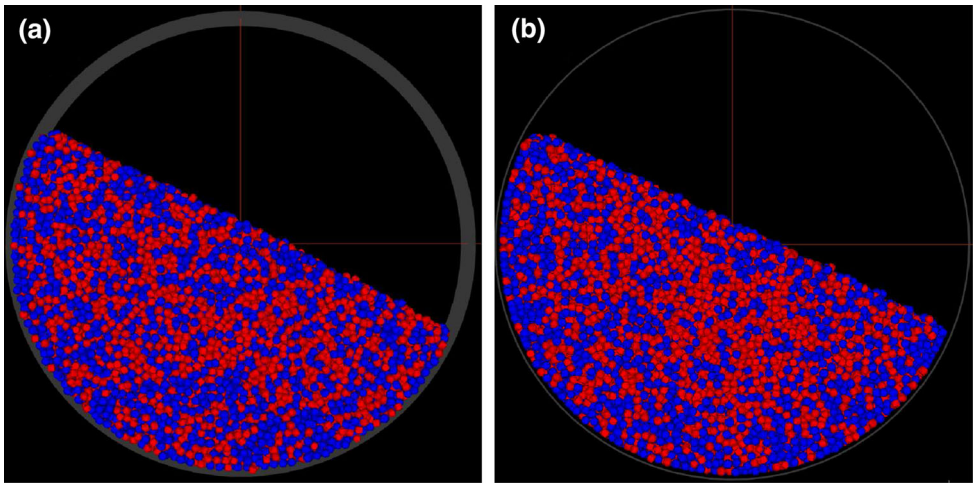

Fig. 5 Particle distribution for binary mixture with particle shape factors of 2.03 (*blue*) and 2.55 (*red*) at two stages during the cylinder's rotation: **a** after 4.5 rotations and **b** after 9 rotations (color figure online)

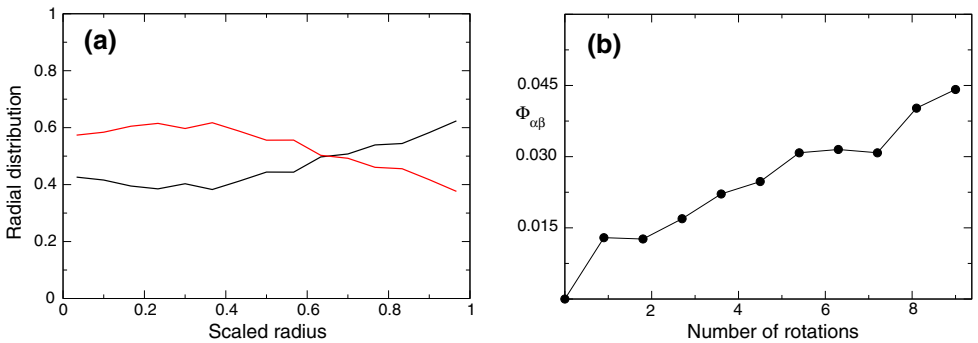

Fig. 6 **a** Radial distribution function for binary particle mixture with $R_n = 1.256$. **b** Segregation measure as a function of number of rotations for a binary particle mixture with with $R_n = 1.256$ (color figure online)

continuous flow regime, the results are qualitatively similar to that at 3 rpm. In Fig. 7 the variation of the segregation measure is plotted with respect to increasing shape factor ratio, R_n, for the two different rotation rates (1 and 3 rpm). The curve corresponding to 3 rpm is always slightly above the 1 rpm curve, which is likely due to the fact that in a given period of 180 s, the 3 rpm cases completed more rotations and so achieved slightly better segregation. The curves suggest that this measure will asymptote towards a value of approximately 0.5, for very large R_n.

4 Segregation mechanism

In our bi-disperse mixture, we have used particle densities and average sizes which are the same (for the two particle types) so as to eliminate segregation due to these properties (*viz.* buoyancy and percolation). The DEM simulations just presented have clearly shown that there is segregation between the two particle types with spherical particles going to the periphery of the cylinder and (more) cubical particles found predominantly in the inner (core) region. We

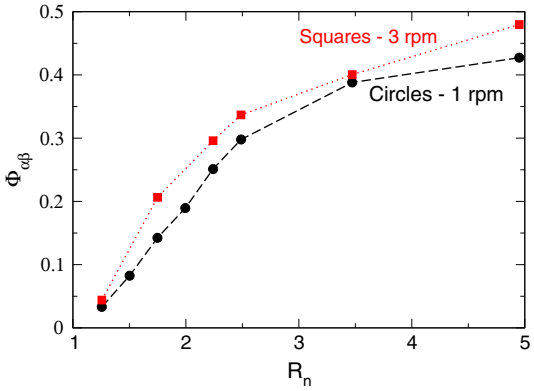

Fig. 7 Segregation measure $\phi_{\alpha\beta}$ at the end of each simulation run versus shape factor ratio, R_n for the two cylinder rotation speeds we have simulated. This measure appears to asymptote to a value of around 0.5 (for large R_n) (color figure online)

now attempt identify the main segregation mechanism which drives this segregation.

To do this we will present data from the DEM simulations on firstly the speed of the different particle shape-types in the free flowing surface layer and secondly particle trajectories (for both particle types). Based on this data, we will then elucidate the driving mechanism for segregation.

4.1 Surface particle speeds

To determine the average surface speed of the two particle shape-types we implemented the following procedure. The circular cross-section of the tumbler was divided into ten vertical, rectangular boxes. The diameter of the cylinder is 10 cm and since each box has the same width, this width is 1 cm or five particle diameters. The highest (i.e. largest y value) ten particles in each box of each particle shape-type are then identified. The speeds of these 100 particles (of each shape-type) are then averaged. The difference in speeds between the two particle shape-types is then calculated, at each DEM time-step. From this three important quantities characterize the difference in surface particle speeds. (i) The percentage of time one particle shape-type has a larger speed than the other shape-type. If the particle shape-types have (roughly) the same average surface speed then this would be approximately 50/50. However if one particle shape-type has a consistently larger average surface speed than the other, this will be more like 70/30, or more extreme if the difference is more consistent. We denote this measure as $T_{S>C}$ and is quoted as a percentage (of time). (ii) The average differential speed between the two particle shape-types averaged over 10,000 consecutive DEM time-steps. The average DEM time-step is around 10^{-5} s, so this averaging period is about 0.1 s. We denote this measure as ΔV. (iii) The average spread in the average differential speed, i.e. the variance of the average differential speed. This gives us an indication if there are large fluctuations about the average difference or if this difference is consistently larger for one shape-type over the other. This measure is denoted as σ_V. As this is a computationally expensive procedure, we apply it to four select cases. These were all for a rotational speed of 3 rpm and particle size ratios, R_n, of 1.256, 1.995, 3.472 and 4.951.

The surface speeds of the two particle shape-types (cubical and spherical) for the shape factor ratios $R_n = 1.256$ and 4.951 are shown in Fig. 8. The black coloured curves are results for the spherical particles while the red coloured curves are for the more cubical particles. One can see in Fig. 8 that the (averaged) speed (for each shape-type) varies rapidly with the fluctuations in the surface flow region but the speeds are bounded in banded regions around a mean avalanche speed. Over the entire 180 seconds of rotation, one can see for the case $R_n = 1.256$ that there is much more overlapping of the banded regions corresponding to the red and black curves than for $R_n = 4.951$. Over a smaller time period of 5 s (i.e. 40 to 45 s, see Fig. 9) one can clearly see the spherical particles have a larger averaged surface speed than the more cubical particles for $R_n = 4.951$ (compared to $R_n = 1.256$). Qualitatively it therefore appears the spherical particles have a consistently larger averaged surface speed than the more cubical particles.

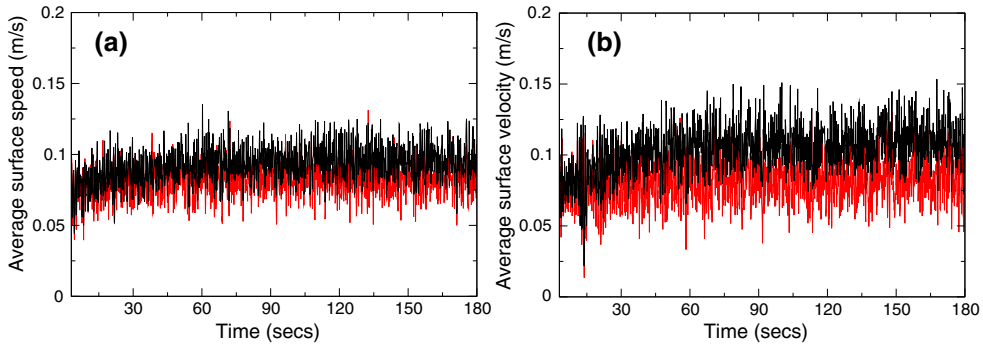

Fig. 8 The average surface speeds of more cubical particles (*red*) and spherical particles (*black*) for **a** $R_n = 1.256$ over 180 s. **b** $R_n = 4.951$ over 180 s (color figure online)

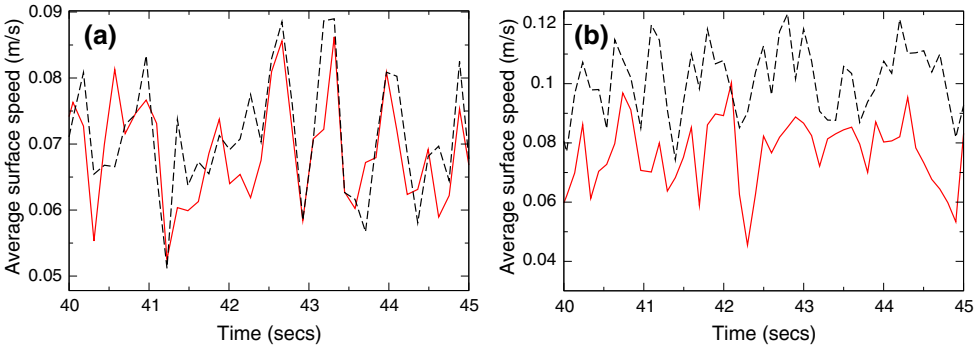

Fig. 9 The average surface speeds of more cubical particles (*red*) and spherical particles (*black*) for **a** $R_n = 1.256$ from 40 to 45 s and **b** $R_n = 4.951$ from 40 to 45 s (color figure online)

We now quantitatively analyse these results by tabulating the three measures detailed above for each of the four particles size ratios. These are shown in Tables 2 and 3. Table 2 gives results for the period of 3 to 83 s when the most rapid segregation occurs. (Note, in the first 3 s of rotation, the particle bed moves as a rigid body until the angle of repose is reached, so we don't include this period in the surface averaging.) In each case the spherical particles travel faster along the top surface (on average) compared to the more cubical particles. For $R_n = 1.256$, this percentage of time is around 59% while for the $R_n = 4.951$ it is almost 95%. So this means for $R_n = 4.951$ for almost the entire duration of time the spherical particles travel faster down the free surface than the more cubical particles. The differential in speed between the spherical and cubical particles provides quantitative evidence that the spherical particles travel significantly faster down the free surface compared to the more cubical particles. For $R_n = 1.256$ this differential is 1.57 mm/s (in favour of the spherical particles). But for the other cases this difference grows rapidly to 9.4 mm/s ($R_n = 1.995$), 17.36 mm/s ($R_n = 3.47$) and 19.9 mm/s ($R_n = 4.951$). Given that the averaged surface speed of the cubical particles is 75 mm/s (see Fig. 8), these absolute differences represent about 2.1% of the cubical particle surface speed, for $R_n = 1.256$ growing to 26.5% for $R_n = 4.951$. So the difference in surface particle speeds increases by more than a factor of ten as the particle shape factor ratio increases from 1.25 to 4.9.

The last quantity we calculated was the standard deviation in the average surface speed difference, between the two particle types. If this standard deviation is greater than the actual average surface speed, this would indicate large fluctuations. In this case, it would imply a significant fraction of time the particle type which was slower on average might at certain instants actually have a larger speed. Looking at the spread in speeds (column 4 in Table 2) for the smallest size ratio of 1.256 the spread is 6.722 mm/s (compared to an average speed of 1.569 mm/s). Hence at many instants the more cubical particles travel faster along the sloped, top surface than do the spherical particles. Overall, this results in a low segregation (as seen in the first row of Table 1). Conversely, when the shape ratio is large i.e. when $R_n = 4.951$ the spread is 13.37 mm/s which is still smaller than the average speed of 19.9 mm/s. This implies that it is rare for the more cubical particles to travel faster than the spherical particles along the top surface. Correspondingly, this results in a large overall segregation (as seen in the last row of Table 1). So for the larger R_n cases, these results indicate not only do the spherical particles *consistently* travel down the free surface faster than the more cubical particles, they do it with a *significantly* larger surface speed.

To see if these measure changed significantly, the periods over which they were calculated were extended to the entire duration of the simulations (180 s). The results are shown

Table 2 Differences in speeds (spherical particles–cubical particles) of the two particle shape-types on the free surface from 3 to 83 s, for four different shape ratios

R_n	$T_{S>C}$ (%)	ΔV (mm/s)	σ_V (mm/s)
1.256	59.20	1.569	6.722
1.995	85.31	9.452	9.445
3.472	93.91	17.36	11.62
4.951	94.25	19.90	13.37

The second column gives the % of time the spherical particles have a larger speed than the more cubical particles, the third column gives the (averaged) speed difference between spherical and more cubical particles and fourth column gives the spread in this difference. See text for more details on these measures. *Note* for the first 3 s, the particle bed moves as a rigid body until the angle of repose is reached

Table 3 Differences in speeds (spherical particles–cubical particles) of the two particle shape-types on the free surface over complete simulation of 180 s, for four different shape ratios

R_n	$T_{S>C}$ (%)	ΔV (mm/s)	σ_V (mm/s)
1.256	60.39	1.804	6.654
1.995	88.87	11.60	9.746
3.472	95.60	20.84	12.50
4.951	96.06	23.28	13.65

The second column gives the % of time the spherical particles have a larger speed than the more cubical particles, the third column gives the (averaged) speed difference between spherical and more cubical particles and fourth column gives the spread in this difference. See text for more details on these measures

in Table 3 and are generally similar to the first 80 s of the simulation. The percentages of time when the spherical particles have a larger surface speed than the cubical particles is slightly larger over the whole 180 s of rotation. Also the differentials in speeds between the two particle types is slightly larger over the entire simulation. These indicate segregation proceeds throughout the entire nine cylindrical rotations, but tends to slow down in the later rotations.

4.2 Particle trajectories

Next consider particle trajectories as the particles travel around the particle bed in response to the cylinder rotation. We studied a number of trajectories of both spherical and more cubical particles and selected the following two trajectories which are representative of the many trajectories studied. Figure 10a shows a cubical particle trajectory (with $n = 4$). The particle begins close to the cylindrical boundary, as it reaches the head (i.e. top of the free flowing layer, see Fig. 1a) of the particle bed, it travels down the surface layer, but one observes a number of deviations towards the centre core (see arrows in Fig. 10a). It can be clearly seen the cubical particle is forced towards the core region (just below the free flowing surface layer) and does not subsequently enter the toe region. Figure 10b shows a trajectory of a spherical particle, which also begins close to the cylindrical boundary. In contrast to the cubical particle trajectory, this spherical particle takes a semi-circular path around the particle bed with no significant deviations towards the core. These two trajectories are typical of the many cases we have analysed and demonstrate the general trajectories of cubical and spherical particles during the cylinder rotation.

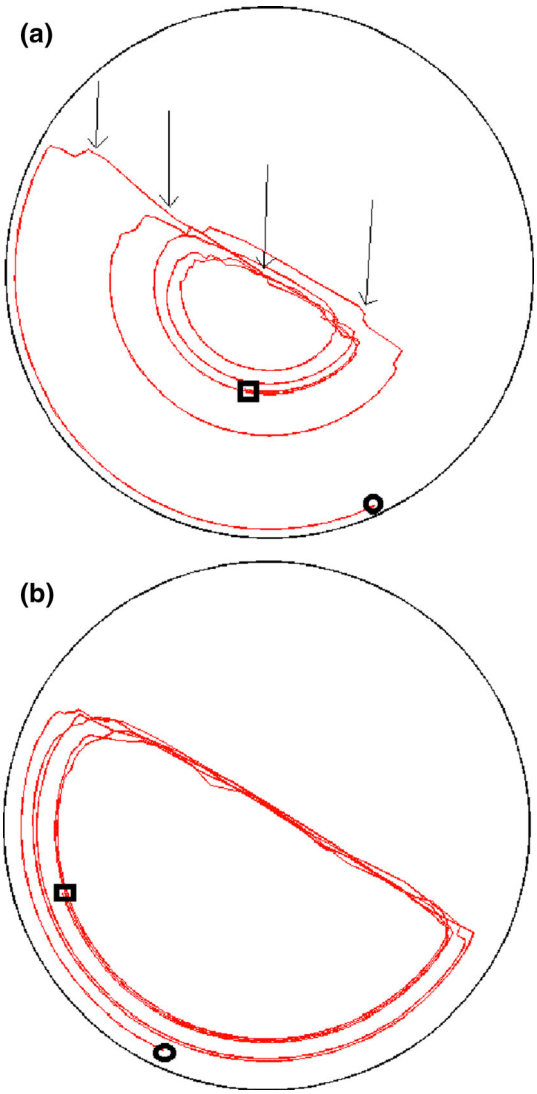

Fig. 10 **a** Particle trajectory of a more cubical particle ($n = 4$) as it travels around the particle bed. *Arrows point* to deviations of the trajectory which force the particle into the core region. The *circle* shows where the particle began and the *square* where it finishes. **b** Particle trajectory of a spherical particle as it travels around the particle bed. *Note* the absence of significant deviations towards the core region, as the particle flows along the surface layer (color figure online)

4.3 Mechanism: particle flowability

It is conjectured here that the primary mechanism for segregation is a larger and faster dissipation of energy for more cubical particles compared to spherical particles as they travel down the free flowing surface layer. This is manifested in our DEM data as different surface speeds for the two particle shape-types, i.e. a significantly larger surface speed for spherical particles when compared to more cubical particles. We call this mechanism particle *flowability*—the rounder particles have better flowability (i.e. lower resistance to flow which results in slower energy dissipation) than the less rounded particles.

As particles reach the head of the particle bed, after being rotated through rigid body motion, both particle shape-types are initially at the same location, so that they have the same potential energy. Once they start traveling down the surface layer, they convert this potential energy into kinetic energy. They remain mobile in the surface layer as long as their kinetic energy is positive. This will occur as long as they do not dissipate all their kinetic energy through frictional interactions and the inelasticity of the collisions with surrounding particles. However, if they do dissipate all of their kinetic energy, they come to rest at some point along the surface layer, whereupon other particles will move past/over them.

Thus the key control for the distance a particle travels down the free surface is the energy dissipation rate of that particle. The energy dissipation rate is dependent on the particle shape with increasingly non-round particles having increasingly higher dissipation. This was shown by Cleary [32] when examining Couette shear flow for granular particles with a

variety of shapes. So the increased blockiness of a particle causes the supply of energy to be consumed more quickly and so the distance it travels down along the surface layer is shorter.

There is a minimum kinetic energy needed to maintain a fluidised behaviour. Once this threshold is reached, it leads to the deposition of the slowest and lowest moving particles out of the shear zone (into the core region) which effectively become frozen in place as was previously demonstrated by Cleary [33]. Cubical particles which are deposited into the core, are passed over by faster moving particles and hence experience a downwards pressure, forcing these particles deeper into the core. This is seen explicitly in the cubical particle trajectory (see Fig. 10a) with a number of downward deviations of the particle from the surface layer into the core. Over subsequent cylinder rotations, this leads to a progressively larger fraction of the cubical particles being buried below the surface layer and hence a larger core of cubical particles evolves.

An implication of this mechanism, based on the DEM data, is that segregation occurs slowly (more slowly than for percolation and buoyancy). For density and size segregation [8,9] segregation occurs rapidly-roughly within one to two rotations. As can be seen in Figs. 2b and 4b, segregation based on shape differences occurs over a period of 5–10 rotations. The amount of segregation increases with each rotation due to additional deposition of particles from the head of the bed onto the core region, which slowly deposits more cubical particles in the core region and forces them down.

4.4 Further discussion

It is important to put our work in context of other related works. Wachs et al. [26] using DEM simulations observed that the top surface of their rotating granular bed may not remain planar. There, for increasingly angular particles, such as cylinders, cubes and tetrahedrons the top surface took up an S-shape, while at the same rotation rate with spheres the top surface was flat. Those simulations were run at a larger rotation rate of 65 rpm with a cylinder radius of 50 mm, yielding a Froude number of 0.24 so that the flow may have entered the cataracting regime. We have also previously observed a non-planar top surface [9] for mixtures of cubical and spherical particles. However, in that case, although the rotation rate was similar to this work (around 1 rpm) the cylinder was very short in length in the axial direction which we argued contributed to a non-planar interface. When the cylinder has a small axial length, packing of particles at the end-walls becomes dominant—the particles tend to get wedged (or packed) tightly between the two planar ends. This contributes to a higher angle of repose near the head of the bed, e.g. see Fig. 2b in reference [9]. In the present simulations, which are carried out in a long cylinder in the continuous flow regime (for flow rate) we have not observed any significant deviation of the top surface from planar. This means both particle shape-types begin from the same position at the head of the bed.

Makse [25] explained stratification patterns seen in experiments in a Hele-Shaw cell [23,24] through differing angles of repose for the two shape types. While cubical particles will form heaps with larger angles of repose compared to heaps formed from spheres, it appears this is not relevant to the problem we are investigating here. For the case investigated in our present study, the head region consists of a mixture of spherical and more cubical particles and thus the top surface remains flat rather than the bent interface of Makse (see Fig. 1b of reference [25]). Presumably, if the angle of repose effect that Makse has outlined was important here then the more cubical particles would begin to avalanche down the free surface from a higher position than the spherical particles. This would imply that the cubical particles would have a larger velocity along the flowing layer, in comparison to the spherical particles, which is in contradiction to our average surface velocity results (above). Rather we have seen it is the rounder particles which move faster along the flowing layer (i.e. better flowability) which is related to their slower energy dissipation compared to cubical particles.

Finally we return to the question of the choice of size equivalency for the different shapes. As outlined in Sect. 2, we have used the inscribed sphere (which is within a cubic particle) as being equivalent in size to a cubic one.

We now analyse the possible effects of this choice. As the inscribed sphere is entirely enclosed within the corresponding super-quadric particle, the main risk is that it will behave as if it is dynamically smaller than the more cubical particles. This could introduce a component of size segregation due to the spheres behaving as if they were dynamically smaller. If such segregation were occurring due to particle size differences, we would expect the spheres to segregate to the core of the particle bed and the more cubical particles to segregate towards the cylinder walls. However, this is opposite to what is observed, i.e. the more cubical particles are found to migrate towards the core. So if there is any size effect occurring this would in fact be in the opposite direction and lead to understating the magnitude of the shape segregation. It seems extremely unlikely that the dynamical equivalent sphere could be smaller than the one used here. On this basis the observed shape segregation effects cannot be a consequence of misinterpretation of size effects.

Whilst the choice of the equivalent sized sphere (inscribed, equal volume or circumscribed) is still a point of some conjecture, we believe our results clearly show that shape is the cause of segregation observed in this paper. From the data presented, with increasing sharpness of the super-quadric particle corners, i.e increasing n, the speed differential (of the surface layer particles) between more cubical particles

and spheres increases. This can only be attributable to particle shape.

By how much this shape segregation would be enhanced if using dynamical volume equivalency or cicumscribed spheres, we cannot currently determine from the present study. However, it is on balance likely that shape segregation will still be a weaker effect than are either size or density segregation (in terms of rate and extent of segregation or of the kinetics that lead to this occurring). Understanding the dynamical equivalency of different shaped particles will continue to be an important issue, not only for segregation but for any system where particles of different shapes need to be compared quantitatively.

5 Conclusions

When a granular mixture composed of two types of particles (spherical and more cubical) is rotated slowly in a cylindrical tumbler, the more cubical particles are found to segregate to form an inner core leaving the more rounded particles concentrated near the cylinder wall. The segregation occurs along the top, free surface of the granular mixture and is driven by the difference in the rate of energy dissipation of the two particle shape-types which we call particle *flowability*. More cubical particles, with their sharper corners, tend to dissipate their energy more rapidly and hence move more slowly as they travel down the free surface. This was demonstrated explicitly when comparing the speeds of spherical and more cubical particles in the flowing layer. The spherical particles reach the bottom end of the flowing layer and are then transported around the cylinder through rigid body motion.

The more cubical particles, due to higher energy dissipation than the spherical particles, come to rest along and below the flowing layer (not making it to the toe region). At this point they are deposited out of the flowing layer into the core and as other particles move over them in the flowing layer get pushed further and further into the core. Hence the more cubical particles become buried and concentrate to the center of the bed. Subsequent cylinder rotations reinforce these events, leading to segregation which increase asymptotically to a maximum $\phi_{\alpha\beta}$ of about 0.5.

It is instructive to compare the segregation due to particle shape with size and density segregation, which have been well studied and whose mechanisms are now well accepted.

- Shape segregation is much weaker than both size and/or density segregation. The maximum value of the overall segregation measure ϕ_{AB} only reached about 0.5, while for density and size segregation this measure reaches up to 0.8–0.9. Moreover, segregation in localized areas is never complete - any small region in the particle bed will have both types of particles present. In contrast, in both size and density segregation local regions of the particle bed (i.e. near cylinder wall or in the core) can be almost devoid of the other particle type.
- The kinetics are much slower for shape segregation compared to size and/or density segregation. It takes of the order of 5–10 rotations of the tumbler before the (asymptotic) steady state is reached. In contrast for size and/or density segregation, it only takes 1–2 rotations of the tumbler. This observation correlates with the weakness of the shape segregation mechanism, mentioned above.
- Segregation occurs *along* the flowing layer rather than *through* the flowing layer as with size and/or density segregation.
- In shape segregation, the interface between the segregated domains tends to be rather diffuse or fuzzy, while for size and/or density segregation it is quite well defined.

We have specifically focused in this paper on binary mixtures of more cubical particles and spherical particles. However, based on this work we make some more (general) predictions on other granular mixtures where the particles differ in their flowability (or speed) along an inclined surface. This difference would be related to the effective roughness of the surfaces of the particles. Roughness has contributions from both coarse scale structures and finer scale structures (friction). So if we had mixtures of faceted particles and less faceted particles we would expect the less faceted particles to flow more easily along the top surface. (When we refer to faceted particles we imply an irregular shaped particle with crevices etc.) The more faceted particles could also be expected to segregate to the central core, while the less faceted particles would migrate to the periphery of the cylinder. If we had mixtures of particles with more friction (i.e. rough surfaces) and particles with less friction (i.e smoother surfaces), once again we could expect the rougher particles to flow less easily along the upper free surface. We then expect the rougher particles should segregate to the core and smoother particles to the periphery of the cylinder.

Compliance with ethical standards

Conflict of interest The authors declare that they have no conflict of interest.

References

1. Ottino, J.M., Khakhar, D.V.: Mixing and segregation of granular materials. Ann. Rev. Fluid Mech. **32**, 55–91 (2000)
2. Bridgwater, J., Foo, W.S., Stephens, D.J.: Particle mixing and segregation in failure zones—theory and experiment. Powder Technol. **41**, 147–158 (1985)

3. Savage, S.B., Lun, C.K.K.: Particle size segregation in inclined chute flow of dry cohesionless granular solids. J. Fluid Mech. **180**, 311–335 (1988)
4. Gray, J.M.N.T., Ancey, C.: Multi-component particle-size segregation in shallow granular avalanches. J. Fluid Mech. **678**, 535–588 (2011)
5. Gray, J.M.N.T., Thornton, A.R.: A theory of particle size segregation in shallow granular free surface flows. Proc. R. Soc. Lond. A **461**, 1447–1473 (2005)
6. Khakhar, D.V., McCarthy, J.J., Ottino, J.J.: Radial segregation of granular mixtures in rotating tumblers. Phys. Fluids **9**, 3600–3614 (1997)
7. Boutreux, T., de Gennes, P.G.: Surface flows of granular mixtures: I. General principles and minimal model. J. de Phys. I **6**, 1295–1304 (1996)
8. Pereira, G.G., Sinnott, M.D., Cleary, P.W., Liffman, K., Metcalfe, G., Šutalo, I.D.: Insights from simulations into mechanisms for density segregation of granular mixtures in rotating cylinders. Granul. Matter **13**, 53–74 (2011)
9. Pereira, G.G., Pucilowski, S., Liffman, K., Cleary, P.W.: Streak patterns in binary granular media in a rotary classifier. Appl. Math. Model. **35**, 1638–1646 (2011)
10. Fan, Y., Schlick, C.P., Umbanhowar, P.B., Ottino, J.M., Lueptow, R.M.: Modelling size segregation of granular materials: the roles of segregation, advection and diffusion. J. Fluid Mech. **741**, 252–279 (2014)
11. Tunuguntla, D.R., Bokhove, O., Thornton, A.R.: A mixture theory for size and density segregation in shallow granular flows. J. Fluid Mech. **749**, 99–112 (2014)
12. Marks, B., Rognon, P., Einav, I.: Grain-size dynamics of polydisperse granular segregation down inclined planes. J. Fluid Mech. **690**, 499–511 (2012)
13. Pereira, G.G., Cleary, P.W.: Radial segregation of multi-component granular media in a rotating tumbler. Granul. Matter **15**, 705–724 (2013)
14. Pereira, G.G., Tran, N., Cleary, P.W.: Segregation of combined size and density varying binary granular mixtures in a slowly rotating tumbler. Granul. Matter **16**, 711–732 (2014)
15. Arntz, M.M.H.D., Beeftink, H.H., den Otter, W.K., Briels, W.J., Boom, R.M.: Segregation of granular particles by mass, radius and density in a horizontal rotating drum. AICHE J. **60**, 50–59 (2014)
16. Fan, Y., Hill, K.M.: Shear induced segregation of particles by material density. Phys. Rev. E **92**(2), 1–9 (2015)
17. Santos, D.A., Barrozo, M.A.S., Duarte, C.R., Weigler, F., Mellmann, J.: Investigation of particle dynamics in a rotary drum by means of experiments and numerical simulations using DEM. Adv. Powder Technol. **27**, 692–703 (2016)
18. Schlick, C.P., Fan, Y., Umbanhowar, P.B., Ottino, J.M., Lueptow, R.M.: Granular segregation in circular tumblers: theoretical model and scaling laws. J. Fluid Mech. **765**, 632–652 (2015)
19. Lu, G., Third, J.R., Muller, C.R.: Discrete element models for non-spherical particle systems: From theoretical developments to applications. Chem. Eng. Sci. **127**, 425–465 (2015)
20. Pollard, B.L., Henein, H.: Kinetics of radial segregation of different sized irregular particles in rotary cylinders. Can. Metal. Quat. **28**, 29–40 (1989)
21. Dube, O., Alizadeh, E., Chaouki, J., Bertrand, F.: Dynamics of non-spherical particles in a rotating drum. Chem. Eng. Sci. **101**, 486–502 (2013)
22. Caulkin, R., Jia, X., Fairweather, M., Williams, R.A.: Geometric aspects of particle segregation. Phys. Rev. E **81**(5), 1–9 (2010)
23. Makse, H.A., Havlin, S., King, P.R., Stanley, H.E.: Spontaneous stratification in granular mixtures. Nature **386**, 379–382 (1997)
24. Makse, H.A., Cizeau, H.A., Stanley, H.E.: Possible stratification mechanisms in granular mixtures. Phys. Rev. Lett. **78**, 3298–3301 (1997)
25. Makse, H.A.: Stratification instability in granular flows. Phys. Rev. E **56**, 7008–7016 (1997)
26. Wachs, A., Girolami, L., Vinay, G., Ferrer, G.: Grains3D, a flexible DEM approach for particles of arbitrary convex shape—Part I: numerical model and validations. Powder Technol. **224**, 374–389 (2012)
27. Hohner, D., Wirtz, S., Scherer, V.: A study on the influence of particle shape and shape approximation on particle mechanics in a rotating drum using the discrete element method. Powder Technol. **253**, 256–265 (2014)
28. Cleary, P.W.: Industrial particle flow modelling using the discrete element method. Eng. Comput. **26**, 698–743 (2009)
29. Hayter, D., Pereira, G., Liffman, K., Aldham, B., Johns, S., Šutalo, I., Brooks, G., Cleary, P., Metcalfe, G.: Density segregation of granular material in a rotating cylindrical tumbler, Proceeding of SPIE, **7270**, 727010(1–10), (2008)
30. Pereira, G.G., Cleary, P.W.: De-mixing of binary particle mixtures during unloading from a V-blender. Chem. Eng. Sci. **94**, 93–107 (2013)
31. Cleary, P.W.: Large scale industrial DEM modelling. Eng. Comput. **21**, 169–204 (2004)
32. Cleary, P.W.: The effect of particle shape on simple shear flows. Powder Tech. **179**, 144–163 (2008)
33. Cleary, P.W.: Granular flows fundamentals and applications, Chap. 8, in Granular and Complex Materials, World Scientific Lecture Notes in Complex Systems (eds: T. Aste, T. Di Matteo and A. Tordesillas), **8**, 141–168, (2007)